

Power uprates
and plant life extension

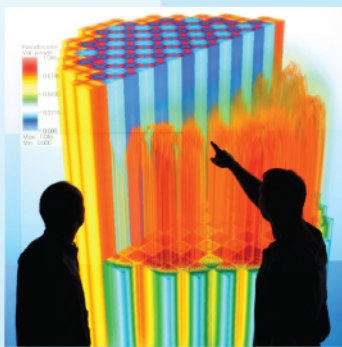


CASL-U-2014-0028-000



Consortium for Advanced Simulation of LWRs

Engineering design
and analysis



Milestone Report L2:VUQ.SAUQ.P5.01

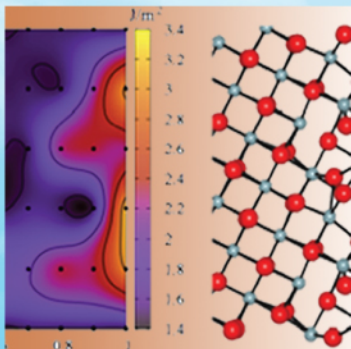
Development of Hybrid Order Reduction Methods for Uncertainty Quantification

Science-enabling
high performance
computing



Hany Abdel-Khalik,
Ralph Smith,
Clayton Websters

Fundamental science



North Carolina State University
Departments of Nuclear Engineering and
Mathematics

September 30, 2013

Plant operational data



U.S. DEPARTMENT OF
ENERGY

Nuclear Energy

CASL L2 Milestone Report

Development of Hybrid Order Reduction Methods for Uncertainty Quantification

L2:VUQ.SAUQ.P5.01

Principal Investigators:

Hany Abdel-Khalik

Ralph Smith

Clayton Websters

Contributors:

Youngsuk Bang,

Jason Hite

Zhengzheng Hu

C.T.Kelley

M. Stoyanov

Jeffrey Willert

North Carolina State University
Departments of Nuclear Engineering and Mathematics

September 30th, 2012

Executive Summary:

This milestone investigates the use of recently developed hybrid methods to enable the management of uncertainties throughout reactor models. Employing the state-of-the-art methods in their current form, e.g. variational methods or sampling methods, is expected to be impractical for realistic reactor models. This follows because nuclear models are often nonlinear, multi-physics, and associated with many input parameters and responses of interest. The developed hybrid approach aims to combine existing methods for uncertainty management in an effective way to overcome their limitations. Past year has focused on presenting the basic idea behind the hybrid approach, that's to employ variational methods to calculate first order derivatives of single physics model's responses with respect to its input parameters. By appropriately sampling these derivatives one can reduce the effective dimensionality of the parameter space for the overall model. Linear algebra operations identify active subspaces at the interface between each two physics models. The premise is that the subspaces identified capture the most dominant effects with the inactive components considered negligibly small. This approach may be considered a generalization of the Karhunen-Loeve expansion used for dimensionality reduction in the context of uncertainty quantification. The KL approach takes advantage of correlations between parameters prior uncertainties, whereas our new approach takes advantage of both prior uncertainty correlations and sensitivities of quantities of interest.

In this fiscal year, a new milestone was initiated to further develop this approach to address realistic reactor models. In particular, we focused on extension of the approach to nonlinear models. This follows as most of the physics feedback effects are expected to lead to nonlinear behavior. Second, we investigate the use of a group of methods developed in the mathematics community aiming at dimensionality reduction, referred to as HDMR techniques, or high dimensional model reduction techniques. Third, we focused on developing a rigorous mathematical representation for the approximation errors resulting from the hybrid approach. The main accomplishments enabled by this work are as follows and are described in the subsequent three chapters:

- 1- Hybrid Subspace methods have been extended to account for nonlinear behavior, by identifying a subspace that captures the nonlinear features of the model (Bang and Abdel-Khalik).
- 2- The use of HDMR techniques is investigated for neutronics problems for possible hybridization with subspace methods (Zhengzheng and Smith).
- 3- Rigorous mathematical error bounds on the responses of interest have been developed for the general nonlinear non-Gaussian case (Stoyanov and Webster).

This work concludes that although nuclear models are nonlinear and high dimensional, a characteristic that cripples existing uncertainty algorithms from being applied effectively for routine engineering analyses, the use of hybrid subspace methods has proven to provide a valuable tool that can reduce the effective dimensionality to a level where existing uncertainty methods become a viable option for use in exhaustive/routine engineering analyses. Different numerical experiments have been carried out to verify

each of the above three developments, both based on simplified models and complicated models used in realistic nuclear engineering calculations. Given these promising results, we believe hybrid subspace methods are ready for deployment into CASL advanced codes to enable uncertainty quantification and data assimilation, which we propose to be the focus on next two fiscal years.

Section 1: Extension of Hybrid Reduced Order Modeling for Nonlinear Models

Introduction:

Reduced order modeling (ROM) has been recognized as an indispensable approach when the engineering analysis requires many executions of high fidelity simulation codes. It identifies patterns in the behavior of the system and approximates the model in lower dimensional form. The primary objective boils down to seek *a minimal size of basis* that captures all possible variations. Several approaches have been proposed for ROM of a single code. As an extension, we address a ROM for multi-physics problems in which several codes are coupled through data transfer. The multi-physics problem would be more challenging; 1) because several codes should be executed, the available execution of each code for ROM would be more limited with respect to overall computational cost; 2) due to multiple physics, the total number of variables to be considered would increase, which requires several ROM on different levels. In this summary, we introduce the *intersection subspace* approach to render *efficient reduced order modeling for multi-physics problems* and numerically demonstrate that *further reduction* can be achieved on the data streams transferred between the different physics codes without compromising the overall accuracy of the coupled simulation.

Theory & Algorithm:

Suppose a model which takes input parameters and produces output responses. The main idea of the ROM approach is reducing the dimensionality by projecting the model onto the so-called *active subspaces*. To efficiently construct the orthonormal basis of the active subspace, we use the randomized range finder, which is originally devised for accelerating a matrix low-rank approximation. Its most important advantage is to make the best of parallel computing platform; thus, the process of the reduced order modeling itself which requires repetitive code executions can be conducted efficiently. Based on the idea of the randomized range finder, different ROM approaches have been proposed depending on where the reduction is rendered. By identifying the *intersection of the active subspaces*, further reduction would be achieved.

Randomized Range Finder:

The randomized algorithms utilize the random input perturbations to identify the sample range. To illustrate the range finding algorithm with random samples, suppose the problem of finding basis for the range of a matrix \mathbf{A} with an exact rank k , which can be mathematically formulated by finding a matrix with k orthonormal columns such that

$$\|\mathbf{A} - \mathbf{Q}\mathbf{Q}^T\mathbf{A}\|_2 \leq \varepsilon \quad (1.1)$$

where ε is a positive error tolerance and the range of \mathbf{Q} is a k -dimensional subspace that captures most of the action of \mathbf{A} . Repeat a process of drawing random vector \bar{x} of which entries are randomly generated and forming the product $\bar{y} = \mathbf{A}\bar{x}$:

$$\bar{y}^{(i)} = \mathbf{A}\bar{x}^{(i)}, \quad i = 1, \dots, k \quad (1.2)$$

Owing to randomness, one can assume that the randomly generated vectors $\bar{x}^{(i)}$ for $i = 1, \dots, k$ are linearly independent and resulting vectors $\bar{y}^{(i)}$ for $i = 1, \dots, k$ are also linearly independent. By linear algebra, the vectors $\bar{y}^{(i)}$ for $i = 1, \dots, k$ spans the range of the matrix \mathbf{A} ; thus, the orthonormal basis of range of the matrix \mathbf{A} can be constructed by orthonormalizing the vectors $\bar{y}^{(i)}$ for $i = 1, \dots, k$. With standard Gaussian random vectors and s extra samples for basis verification, the constructed basis \mathbf{Q} satisfies the following statement with probability at least $1 - 10^{-s}$ [Halko, 2011]:

$$\|(\mathbf{I} - \mathbf{Q}\mathbf{Q}^T)\mathbf{A}\|_2 \leq 10 \sqrt{\frac{2}{\pi}} \max_{i=1, \dots, s} \|(\mathbf{I} - \mathbf{Q}\mathbf{Q}^T)\mathbf{A}\bar{z}^{(i)}\|_2 \quad (1.3)$$

Reduced Order Modeling in Two Levels!

Suppose a single physics model which takes input parameters \bar{x} and produces output responses \bar{y} . Different approaches can be performed depending on where the reduction is rendered and those can be categorized into two groups: *output-level* reduction and *input-level* reduction

In the output-level reduction, the active subspace basis construction via the randomized range finder is straightforward because the information of the active subspace is directly accessible, i.e. the vector to be reduced itself spans the range of the active subspace. It can be considered as identifying patterns in samples. Note that once the basis of the range of \mathbf{A} is constructed as a matrix \mathbf{Q}_o , the vector of the output responses \bar{y} can be transformed to $\bar{y} = \mathbf{Q}_o \mathbf{Q}_o^T \bar{y} = \mathbf{Q}_o \bar{\beta}$. Because the basis can be constructed simply by orthonormalizing the samples (snap-shot method [Holmes, 1996]), it is obvious that this procedure would be applicable to both of linear and nonlinear models. The most of ROM applications have been implemented on this level.

In the input-level reduction, the range of input parameters is not directly accessible unless the model is explicitly known. Instead, we have been shown that the first order derivatives of pseudo¹ responses with respect to inputs at random points span the active subspace of input parameters [Bang, 2012]. The first order derivatives can be most efficiently with adjoint sensitivity analysis which is the well-recognized method in reactor physics community. Then, the basis for input parameters can be identified by orthonormalizing the first order derivatives at random points. Once the active subspace basis of the input parameters is constructed as a matrix \mathbf{Q}_i , the vector of input parameters \bar{x} can be transformed to $\bar{x} = \mathbf{Q}_i \mathbf{Q}_i^T \bar{x} = \mathbf{Q}_i \bar{\alpha}$.

Note that the active subspaces for two levels have different meaning. The active subspace of output responses, i.e. \mathbf{Q}_o can be considered as *patterns in their variations*

¹ A pseudo response is a random linear combination of the model's responses. See Ref [1] for more details on its construction.

due to input parameter perturbation. In other words, the outputs can be represented with those patterns. ROM on output-level is taking the only dominant patterns. On the other hand, the active subspace of input parameters, i.e. \mathbf{Q}_I , can be interpreted as their *sensitivity on output response changes*. The premise is that all parameter variations that are orthogonal to the active subspace produce negligible response change. ROM on input-level is taking the only high sensitive components.

Intersection Subspace for Coupled ROM:

We can extend the approaches to handling codes consisting of serially coupled two physics codes where the outputs of one code are passed as inputs to the next code in the chain. Note that data stream between two codes can be simplified as *transferring patterns* which is determined by the former code. Then, the only sensitive components of transferred data to the latter code can contribute to the final output responses. In other words, among the delivered patterns, the only sensitive components need to be considered. There can be two different ROMs; one for taking dominant patterns and one for taking high sensitive components. Focusing on the fact the some variations in dominant patterns may not be influential to the responses changes (in-sensitive), we define the intersection subspace capturing *large variations* AND *high sensitivities*. It is natural to think that the size of the intersection subspace would be smaller than any of separate subspaces. Intuitively, if more active subspaces are involved (more coupled codes), the size of intersection subspace confining all the active subspace would be smaller. This induces the promising perspective that the further reduction would be achievable as more codes are involved.

Constructing the intersection subspace basis can be divided into two stages:

Proto-Algorithm: Intersection Subspace Basis Construction

Given two coupled codes, this procedure computes the intersection subspace for intermediate variables transferred from the former code to the latter code.

Stage A) Pattern Identification in Intermediate Variables

- sample the intermediate variables by executing the former code with random inputs
- compute the active subspace basis by orthonormalizing projected samples

Stage B) Intersection Subspace Extraction

- sample the first order derivatives of pseudo responses with respect to intermediate variables at random points
- project the samples onto the subspace of patterns
- compute the intersection subspace basis by orthonormalizing projected samples

Numerical Demonstration:

We take neutronics calculations as an example, whereby resonance and self-shielding calculations represent one physics code, necessary to calculate the effective multi-group cross-sections, before passing them to the next physics code representing transport calculations. The transport code employs the effective cross-sections to solve for any responses of interest, e.g. k-eigenvalue, flux, few-group cross-sections. The depletion code takes the flux to calculate the depleted and transmuted nuclides densities. This sequence of resonance – transport – depletion calculations are repeated at each depletion step. The effective multi-group cross-sections are considered as intermediate variables

and *the active subspace for all possible variations during the entire depletion cycle under different operating conditions is constructed.*

SCALE6.1 is used for simulations and assembly models of two reactor types are considered (**Figure 1**): Peach Bottom Unit 2 Boiling Water Reactor (PB-2 BWR) [Ivanov, 1999] and Watts Bar Unit 2 Pressurized Water Reactor (WB-2 PWR) [Wagner, 2002]. The applicability of reduced order modeling in highly nonlinear cases due to the poison material burnout (Gd-155 & Gd 157) and in case of different fuel enrichments and control rod insertions are examined with PB-2 BWR and WB-2 PWR models, respectively.

Main purpose of this numerical test is to compare the *size of active subspace basis* via intersection subspace approach to single subspace approach for the same precision of reduced order transformation. To examine the size of active subspace, the singular value spectrums of the random samples are compared and the constructed basis vectors are verified by using κ -metric method, i.e. calculate the response changes due to in-active input components. As can be seen in **Figure 2**, the singular value spectrum of the intersection subspace is decaying faster than the one of the single subspace. Note that the singular values can be considered as the importance of the basis. Therefore, the singular value spectrums show that the intersection subspace can confine the effective multi-group cross-sections into smaller dimension at a given precision (fixed-precision problem). Or with a given subspace size, the intersection subspace approach provides more optimal basis (fixed-size problem), which can be more consolidated by **Figure 3**. Note that if the subspace is constructed correctly, the response change due to in-active input components should be very small. With intersection approach, the subspace size of 800 and 2000 would be sufficient for PB-2 BWR and WB-2 PWR, respectively, while not enough for single subspace approach. Though not included in this summary, the basis is verified for scalar fluxes and assembly-homogenized few-group cross-sections via κ -metric test. Considering the precision of ENDF cross-section library and transport solver convergence criteria (10^{-5} for PB-2 BWR and 10^{-4} for WB-2 PWR), the required size of active subspace could be determined and summarized in **Table 1**.

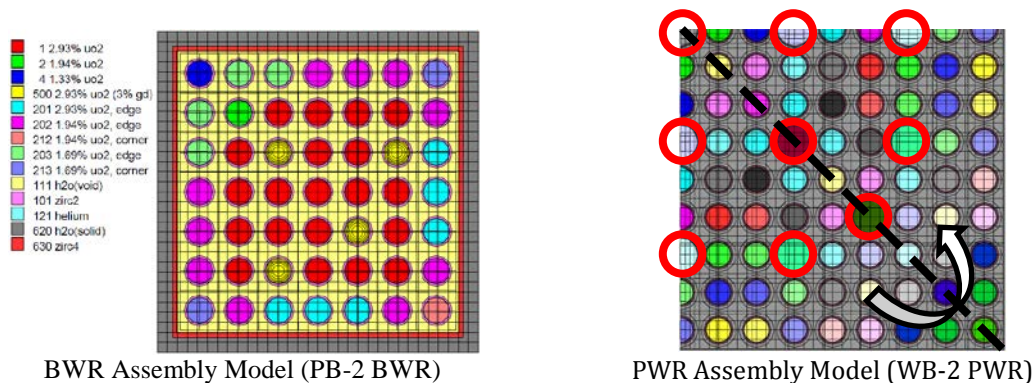
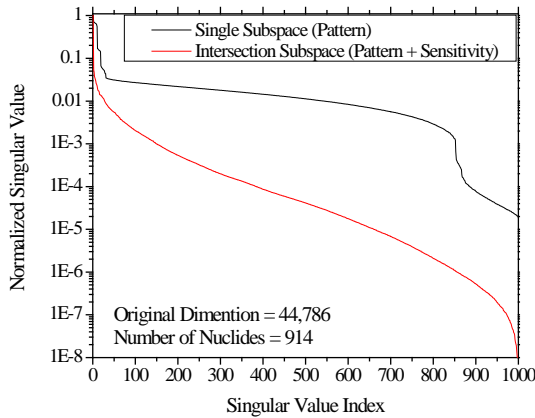
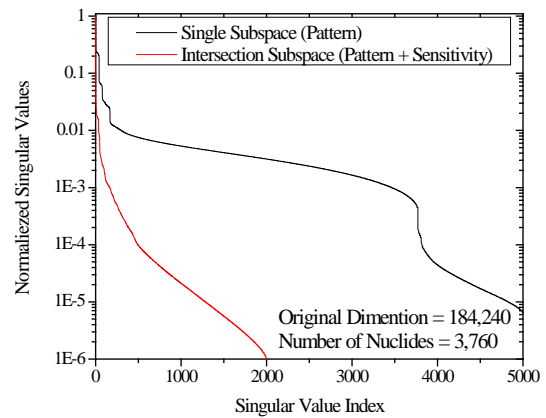


Figure 1. SCALE Assembly (WB-2 PWR) Model

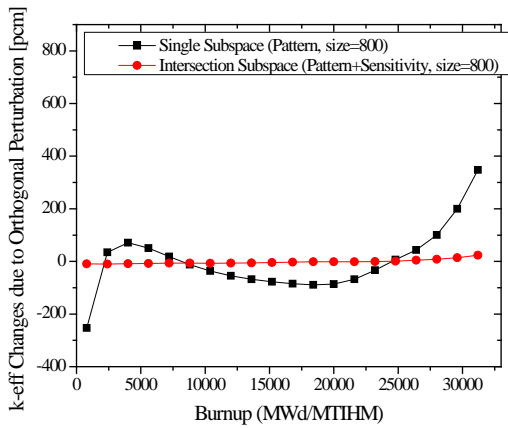


BWR Assembly Model (PB-2 BWR)

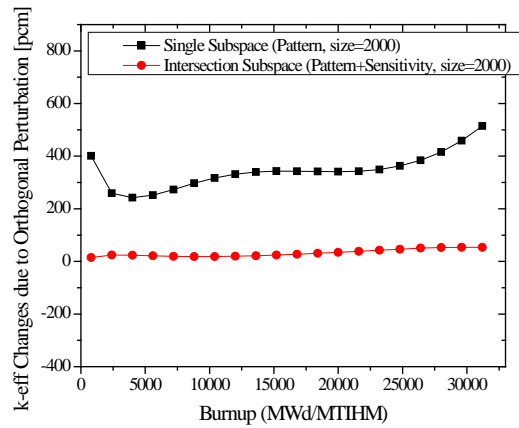


PWR Assembly Model (WB-2 PWR)

Figure 2. Singular Value Spectrum



BWR Assembly Model (PB-2 BWR)



PWR Assembly Model (WB-2 PWR)

Figure 3. κ -metric test for k-eigenvalue
(Active Subspace Size=800 for PB-2 BWR and 2000 for WB-2 PWR)

Table 1. Summary of Test Result

	PB-2 BWR	WB-2 PWR
Original Dimension	44,786	184,240
Reduced Dimension (single subspace, pattern)	1,000 (2.23% of original dim.)	5,000 (2.71% of original dim.)
Reduced Dimension (intersection sub., pattern+sensitivity)	800 (1.79% of original dim.)	2,000 (1.09% of original dim.)

Conclusion:

We show that while each physics code is independently reducible, by appropriately combining the active subspaces from each code using the idea of subspace intersection, further reduction can be achieved. Note that as more codes are coupled, the simulation would become more complicated and computationally intensive, which leads to many engineering analysis impractical. On the other hand, we expect the further reduction as more codes considered, which is very promising to alleviate the computational burden and enhance efficient application of high-fidelity simulation codes.

Section 2: High Dimensional Modeling Reduction Techniques

Introduction:

In (Hu & Smith, 2013), the authors tested the applicability of High-Dimensional Model Representation (HDMR) techniques, originally proposed by (Sobol, 1993), combined with modified Morris screening (Campolongo & Saltelli, 1997) to the homogenized energy model (HEM) for Macro-Fiber Composites (MFC) which has 16 physical parameters. The authors concluded that the proposed algorithm could successfully represent the model with up to 10 parameters which do not have significant high-order (more than 2nd) interactions. Motivated by their findings, we apply the same algorithm to a steady-state, 1-D neutron transport equation which characterizes the dynamics of a group of monoenergetic neutrons travelling in homogeneous planar geometry with isotropic scattering.

As detailed in the general review of (Rabitz & Alis, 1999) and the references cited therein, HDMR techniques have been used to systematically identify the relationships between sets of inputs (e.g., parameters) and outputs (responses). Under the assumption that the effect of inputs on the outputs are independent and cooperative, HDMR expresses the model output as a finite additive sum of correlated functions with increasing numbers of input variables up to the total number of inputs. There are two commonly used expansions: ANOVA-HDMR and Cut-HDMR depending on how the hierarchical functions are evaluated. ANOVA-HDMR, which is often used to analyze global sensitivity, is basically the same as the analysis of variance decomposition (ANOVA). It involves high-dimensional integrations which are computationally expensive to evaluate. Cut-HDMR, on the other hand, depends only on the function values at sample points and thus is more computationally attractive than ANOVA-HDMR. The theoretical foundations of both expansions are detailed in (Rabitz & Alis, 1999).

HDMR was originally proposed as a framework to construct a fully equivalent operational model of complex chemical systems; see (Rabitz & Alis, 1999; Shorter, Precila, & Rabitz, 1999; Wang, Levy II, Li, & Rabitz, 1999; Li, Rosenthal, & Rabitz, 2001). Since its development, it has been used to construct computational models directly from laboratory data, perform quantitative risk assessment, identify key model parameters, analyze global uncertainty, etc. For example, Li et al. (Li, Wang, Rabitz, Wang, & Jaffe, 2002) proposed a framework for global uncertainty assessments using random sampling HDMR (RS-HDMR). They have successfully applied RS-HDMR to

analyze the results of a mathematical model for identifying relevant variables in simulating bioremediation of trace metals/radionuclides in groundwater.

Labovsky and Gunzburger (Gunzburger & Labovsky, 2012) proposed a new methodology to explore the importance of inputs based on Cut-HDMR by examining both individual and pairwise effects. Commonly, when Cut-HDMR expansions are used to approximate the high-dimensional functions, inputs with small individual effect (i.e., outputs do not vary much when inputs have changed) are omitted from the Cut-HDMR expansion starting from the first-order; i.e., such inputs are not considered in high-order terms which account for the interactions among parameters. People often argue that only two inputs with significant separate effect can have important interactions. Labovsky and Gunzburger showed this is not the case for a complex system of PDEs that governs incompressible magnetohydrodynamic flows. The main contribution of that work is to propose a framework to identify/include important interactions between two inputs in the Cut-HDMR when neither of the two inputs is important. Motivated by their work, we will consider the applicability of their framework with some modifications to the 1-D neutron transport equation.

The rest of the report is organized as follows. We first briefly review the 1-D neutron transport equation. The algorithm proposed in (Gunzburger & Labovsky, 2012) is then presented with some modifications. In the Results section, we analyze the applicability of the algorithm on the 1-D transport equation. Concluding Remarks and Future Work is presented in the last section.

1-D Neutron Transport Equation:

We consider a 1-D problem for steady-state, monoenergetic, isotropically scattering neutron transport in homogeneous planar (commonly referred as “slab”) geometry. The governing equation is

$$\mu \frac{\partial \psi}{\partial x}(x, \mu) + \Sigma_t \psi(x, \mu) = \frac{1}{2} [\Sigma_s \phi(x) + Q(x)] \quad (2.1)$$

where $x \in [0, 1]$ and the polar cosine $\mu \in [-1, 1]$. Here $\psi(x, \mu)$ is the azimuthally integrated angular flux, Σ_t is the macroscopic total cross section (\mathbf{m}^{-1}), Σ_s is the macroscopic scattering cross section (\mathbf{m}^{-1}), $\phi(x)$ is the scalar flux; i.e., $\phi(x) = \int_{-1}^1 \psi(x, \mu) d\mu$, and $Q(x)$ is an internal isotropic source.

We assume no incoming flux on the left or right boundaries; i.e., vacuum boundary conditions. The boundary conditions prescribe the incident angular fluxes on the left and right edges of the slab are

$$\begin{aligned} \psi(0, \mu) &= 0 \quad \text{for } \mu > 0, \\ \psi(1, \mu) &= 0 \quad \text{for } \mu < 0. \end{aligned}$$

Eq. 2.1 is solved numerically using a MATLAB code developed by Willert and Kelley². More specifically, the governing equation is represented at a finite set of polar cosine values μ_j with associated weights w_j for $j = 1, \dots, n$

$$\mu_j \frac{\partial \psi_j}{\partial x}(x) + \Sigma_t \psi_j(x) = \frac{1}{2} [\Sigma_s \phi(x) + Q(x)],$$

and the scalar flux is approximated by $\phi(x) = \sum_{j=1}^n w_j \psi_j(x)$. The diamond-difference discretization is used in space, so the angular flux is evaluated at cell-faces. The discretized system is then solved using Source Iteration, or Picard Iteration, during which the scalar flux (part of the source term) is treated explicitly; i.e., evaluated using the angular fluxes at the previous iteration. The scheme at the $(k+1)$ -th iteration is

$$\mu_j \frac{\psi_{j,j+1/2}^{k+1} - \psi_{j,j-1/2}^{k+1}}{\Delta x} + \Sigma_t \frac{\psi_{j,j+1/2}^{k+1} + \psi_{j,j-1/2}^{k+1}}{2} = \frac{1}{2} [\Sigma_s \phi_i^k + Q_i]$$

$$\phi_i^{k+1} = \sum_{j=1}^n w_j \frac{\psi_{j,j+1/2}^{k+1} + \psi_{j,j-1/2}^{k+1}}{2}$$

for $j = 1, \dots, n$ and $i = 1, \dots, N_x$, where N_x is the number of grid points along x .

Motivated by the structure of a typical light water reactor core which typically contains nuclear fuel rods (e.g., uranium, plutonium), control rods (e.g., hafnium, cadmium) and water-filled channels, we consider a material composition shown in Figure 1.



Figure 1. Schematic of the composition of the materials used in the numerical tests.

Cut-HDMR with Screening:

In this section, we briefly summarize the Cut-HDMR expansion. As mentioned previously, Cut-HDMR is more efficient for practical computations since no high-dimensional integrals need to be computed in the expansion. We then introduce the Morris screening which is used to select anchor points for the Cut-HDMR and identify the most influential parameters/interactions. Finally, we present the algorithm that combines the Morris screening with the Cut-HDMR and therefore is able to construct a reduced-order model with both univariate and bivariate effects of parameters.

² <http://www4.ncsu.edu/~ctk/>

Consider a multivariate function $f(\vec{Y}) = f(Y_1, Y_2, \dots, Y_k)$ defined on the k -dimensional domain Ω_k and a pre-chosen anchor point $\vec{Y}^* = (Y_1^*, Y_2^*, \dots, Y_k^*) \in \Omega_k$. The Cut-HDMR takes the form (Rabitz & Alis, 1999)

$$\begin{aligned} f(\vec{Y}) = & f_0 + \sum_{i=1}^k f_i(Y_i) + \sum_{1 \leq i_1 < i_2 \leq k} f_{i_1 i_2}(Y_{i_1}, Y_{i_2}) + \\ & + \sum_{1 \leq i_1 < \dots < i_s \leq k} f_{i_1 \dots i_s}(Y_{i_1}, \dots, Y_{i_s}) + f_{12 \dots k}(Y_1, \dots, Y_k) \end{aligned} \quad (2.2)$$

where

$$\begin{aligned} f_0 = & f(\vec{Y}^*), \quad f_i(Y_i) = f(\vec{Y})|_{\vec{Y}=\vec{Y}^* \setminus Y_i} - f_0, \\ f_{ij}(Y_i, Y_j) = & f(\vec{Y})|_{\vec{Y}=\vec{Y}^* \setminus \{Y_i, Y_j\}} - f_i(Y_i) - f_j(Y_j) - f_0, \dots \end{aligned}$$

The notation $\vec{Y} = \vec{Y}^* \setminus Y_U$ means that the components of \vec{Y} other than those indices that belong to the set U are set equal to those of the anchor point. For example,

$$\begin{aligned} \vec{Y} = \vec{Y}^* \setminus \{Y_i, Y_j\} = \\ = (Y_1^*, \dots, Y_{i-1}^*, Y_i, \dots, Y_j, Y_{j+1}^*, \dots, Y_k^*). \end{aligned}$$

Unlike ANOVA-HDMR, the expansion depends only on function values at the anchor point so that high-dimensional integrations are avoided. This makes Cut-HDMR more attractive for practical computations. However, due to the dependence on the anchor points, the expansion may lead to an unacceptable approximation error. Many efforts have been made to select one or a set of suitable anchor points; see (Ma & Zabararas, 2010) for example. Labovsky and Gunzburger (Gunzburger & Labovsky, 2012) have considered using Morris screening test (Morris, 1991) to identify a set of anchor points, and this will be discussed in the next subsection.

We note that the expansion Eq. 2.2 is exact if all terms are included, though there would be no computational gain. It is often argued that the high-order interactions among inputs are weak and therefore can be omitted from the expansion. In fact, truncating after the second-order interaction terms yields a good approximation (Rabitz, Alis, Shorter, & Shim, 1999; Cao, Chen, & Gunzburger, 2009; Sobol, 2003); i.e.,

$$f(\vec{Y}) \approx f_0 + \sum_{i=1}^k f_i(Y_i) + \sum_{1 \leq i_1 < i_2 \leq k} f_{i_1 i_2}(Y_{i_1}, Y_{i_2}). \quad (2.3)$$

Let us consider a function with 16 parameters. To analyze the sensitivity of the function in terms of the 16 parameters, the most straightforward way is to select grid points in 16-D (e.g., four points in each direction), evaluate the function at the grid points and calculate the numerical derivatives (finite differences). This is, however, computationally impossible, since it involves more than 100 million function evaluations. Furthermore, only 4 points were considered in each direction. If instead the truncated Cut-HDMR is used, only $1 + 4 \times 16 + 4^2 \times \frac{16 \times 15}{2} = 1985$ function evaluations are needed. In other words, if one can afford 300 thousand function evaluations, about 50 grid points can be

considered in each dimension and the 16-D parameter space should be presented reasonably well by those grid points.

Morris Screening:

The tradeoff for the Cut-HDMR being significantly more efficient is that the convergence properties depend on the choice of the reference point. One of the options is to randomly pick points within the domain where the parameters/variables are defined. Following Labovsky and Gunzburger (Gunzburger & Labovsky, 2012), we consider using the modified Morris screening method proposed by Campolongo et al. (Campolongo & Saltelli, 1997) to define a set of anchor points.

Morris screening was originally proposed by Morris (Morris, 1991) to efficiently explore the sensitivity of inputs. Campolongo et al. (Campolongo & Saltelli, 1997) later suggested an improvement aimed at better exploring the input space. Basically, a reference point is randomly selected initially. Through the construction of a sampling matrix, the input space around this reference point is explored/used to evaluate the sensitivity. The unique attribute of the screening procedure is that the sampling matrix provides an “optional” trajectory for calculating the sensitivity (finite difference) of all inputs, so it is the most efficient way to explore the input space. Figure 2 demonstrates a possible trajectory based on the sampling matrix for two inputs.

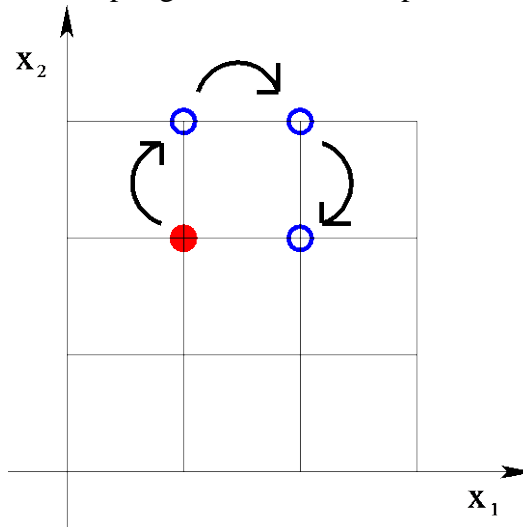


**Figure 2. Sketch of the trajectory in 2D proposed by (Campolongo & Saltelli, 1997).
Dot: reference point; Blue circles: points on the trajectory used to calculate the sensitivity.**

Cut-HDMR with Morris Screening Algorithm:

Motivated by (Gunzburger & Labovsky, 2012) we propose *Algorithm 1* to approximate the k -dimensional multivariate function $f(\vec{Y}) = f(Y_1, Y_2, \dots, Y_k)$ using Cut-HDMR with Morris screening.

Algorithm 1

1. Following the Morris screening method (Campolongo & Saltelli, 1997), construct r first-order sampling matrices $\{\mathbf{B}_\ell^*\}_{\ell=1}^r$ using randomly chosen starting vectors $\{\vec{Y}_\ell^*\}_{\ell=1}^r = [Y_{\ell 1}^*, Y_{\ell 2}^*, \dots, Y_{\ell k}^*]$. These starting vectors are used as anchored points in Cut-HDMR; see step 7.
2. For $\ell = 1, \dots, r$, compute the first-order elementary effect (univariate effect) of $f(\vec{Y})$, $\{d_{ss}^\ell\}_{s=1}^k$, using \mathbf{B}_ℓ^* ; see Appendix.
3. Construct r second-order sampling matrices $\{\mathbf{A}_\ell^*\}_{\ell=1}^r$ using the same starting vectors used for the first-order sampling matrices.
4. For $\ell = 1, \dots, r$, compute the second-order elementary effect (bivariate effect) of $f(\vec{Y})$, $\{d_{sv}^\ell\}_{s,v=1}^k (s \neq v)$, using \mathbf{A}_ℓ^* ; see Appendix.
5. Calculate the mean of elementary effects, \bar{d}_{ij} for $i, j = 1, \dots, k$,

$$\bar{d}_{ij} = \frac{1}{r} \sum_{\ell=1}^r d_{ij}^\ell = \begin{cases} \text{univariate} & i = j \\ \text{bivariate} & \text{otherwise.} \end{cases}$$

6. Screening. Let \mathcal{S}_1 and \mathcal{S}_2 respectively be the set of indexes of the important univariate and bivariate effects, then

$$\mathcal{S}_1 = \left\{ i \mid \frac{\bar{d}_{ii}}{\max(\bar{d}_{ii})} > \epsilon, 1 \leq i \leq k \right\}$$

$$\mathcal{S}_2 = \left\{ (i, j) \mid \frac{\bar{d}_{ij}}{\max(\bar{d}_{ij})} > \epsilon, 1 \leq i, j \leq k, i \neq j \right\},$$

where ϵ is a predefined threshold value.

7. Truncate Cut-HDMR with screening:

$$f(\vec{Y}) \approx f_{cut}(\vec{Y}) = \frac{1}{r} \sum_{\ell=1}^r \left(f_0^\ell + \sum_{i \in \mathcal{S}_1} f_i^\ell(Y_i) + \sum_{(i, j_2) \in \mathcal{S}_2} f_{ij_2}^\ell(Y_{i_1}, Y_{i_2}) \right) \quad (2.4)$$

where

$$f_0^\ell = f(\vec{Y}_\ell^*), \quad f_i^\ell(Y_i) = f(Y_{\ell 1}^*, Y_{\ell 2}^*, \dots, Y_i, \dots, Y_{\ell k}^*) - f_0^\ell,$$

$$f_{ij}^\ell(Y_i, Y_j) = f(Y_{\ell 1}^*, Y_{\ell 2}^*, \dots, Y_i, \dots, Y_j, \dots, Y_{\ell k}^*) - f_i^\ell(Y_i)\delta_i - f_j^\ell(Y_j)\delta_j - f_0^\ell,$$

with

$$\delta_i = \begin{cases} 1 & \text{if } i \in \mathcal{S}_1 \\ 0 & \text{otherwise.} \end{cases}$$

Here only the variables that are significant will be summed in the second term of Eq. 2.4, and only the interactions that are significant will be summed in the third term.

Note that besides the computational cost discussed previously, the screening procedure involves $r(k+1+k^2)$ function evaluations.

Numerical Results:

We now apply Algorithm 1 to test its applicability on the 1-D neutron transport equation. As shown in Figure 1, we consider three different materials (H₂O, U-235 and Hf-177) in 7 sub-regions. Each material has distinctive scattering cross sections and total cross section. To study the sensitivity of these cross sections to the transport equation, values are randomly selected for each region from the predefined domain of the materials. The domain for each material is calculated by perturbing the reported values found in (Sood, Forster, & Parsons, 2003) that are shown in Table 1. The cross sections of Hf-177, however, are calculated using microscopic cross sections (Devaney, Bordwell, & Devaney, 1962) and the number density of Hf-177. The permissible domains of three materials are shown in Table 2. Here the lower/upper bounds for the scattering cross sections are obtained by perturbing the book values by 10%. Since the ratio between the scattering cross section and the total cross section affects the convergence rate of the numerical scheme, to ensure the accuracy of the numerical solution, instead of randomly selecting the total cross sections, the ratios are selected. The lower/upper bounds for the ratios are obtained by perturbing the book values by 2%. The lower/upper bounds of the total cross sections are evaluated from the scattering cross sections and the ratios and are not implemented explicitly in the code. Therefore, the 1-D transport equation has 14 physical parameters (7 scattering cross sections and 7 ratios).

Material	Σ_s	Σ_s / Σ_t	Σ_t
H ₂ O	0.2938	0.9000	0.3264
U-235	0.2481	0.9500	0.2611
Hf-177	0.4500*	0.0829	5.4296*

Table 1. Macroscopic scattering cross sections and total cross sections in (Sood, Forster, & Parsons, 2003). The values for Hf-177 are calculated using the microscopic cross sections (Devaney, Bordwell, & Devaney, 1962) and the number density of the material.

Material	Σ_s	Σ_s / Σ_t	Σ_t
H ₂ O	[0.2644,0.3232]	[0.8820,0.9180]	[0.2880,0.3664]
U-235	[0.2233,0.2729]	[0.9310,0.9690]	[0.2304,0.2931]
Hf-177	[0.4050,0.4950]	[0.0812,0.0846]	[4.7872,6.0961]

Table 2. Lower/upper bounds of the cross sections and ratios of the materials used in the simulations.

We now test *algorithm 1* for accuracy. To evaluate the error of the algorithm, 1000 points were randomly selected in the parameter space to evaluate both the exact and approximated solutions. The angular and scalar fluxes calculated by the model using a randomly selected set of parameters from Table 2 are plotted in Figure 3. Note that the response considered in Cut-HDMR is the integral of the scalar flux over the domain.

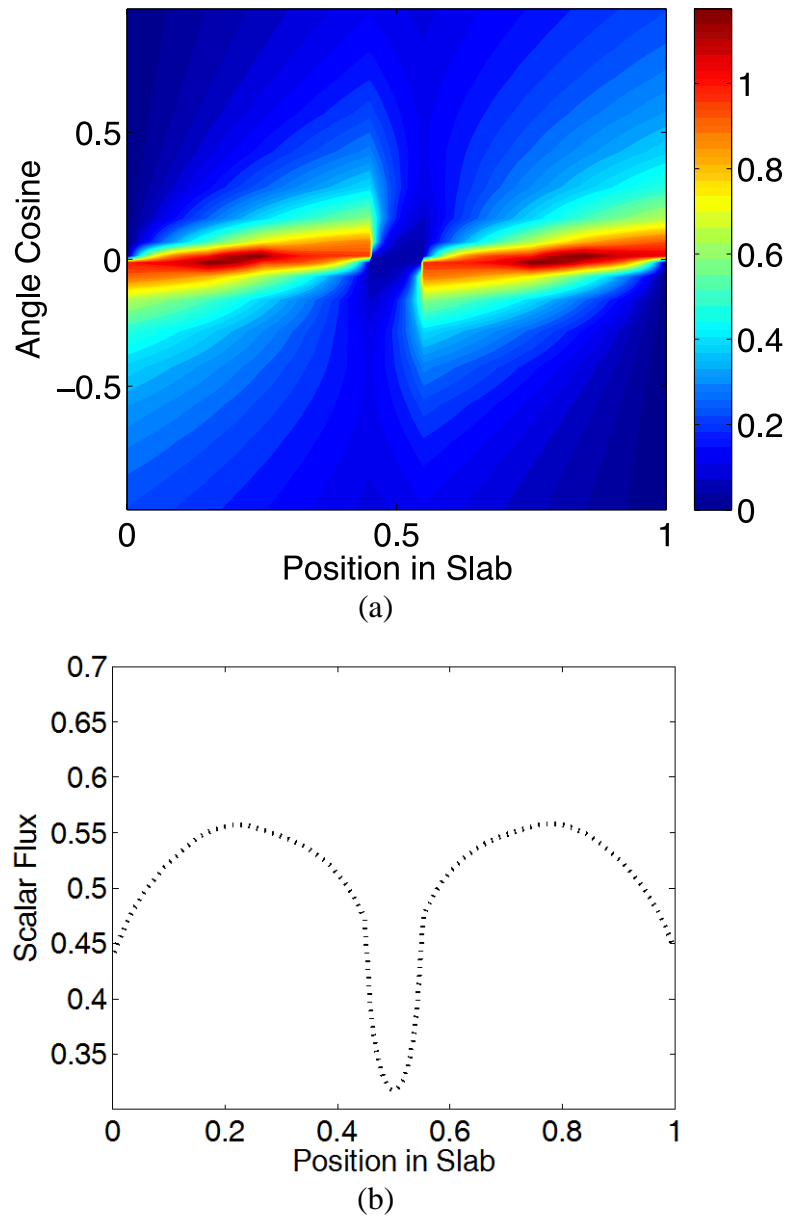


Figure 3. Angular flux (a) and scalar flux (b) calculated by the 1-D transport equation with a randomly selected set of parameters using Table 2.

Five anchor points are selected, 4-level sampling matrices are used, and the threshold value is taken to be 0.05; see Appendix for the definition of a 4-level sampling matrix. The univariate screening finds that only two parameters are not significant at 0.05-level, and these two parameters are the scattering cross sections of U-235 (in the second region from the left) and H₂O (in the third region from the left). Among the 91 pairwise interactions, the bivariate screening finds 13 interactions are not significant. For example, the scattering cross section of U-235 of the second region from the left does not interact with another scattering cross sections, except for the scattering cross section of the H₂O in the first region from the left. We then find that the maximum relative error between the approximation and the exact solution is 4.99% and 67.3% of the evaluation points have

relative error less than 2%. Thus *Algorithm 1* accurately approximates scalar flux of the 1-D neutron transport equation for the material composition shown in Figure 1.

Concluding Remarks and Future Work:

Motivated by Labovsky and Gunzburger (Gunzburger & Labovsky, 2012), we use the modified Morris screening method proposed by Campolongo et al. (Campolongo & Saltelli, 1997) to identify the most influential parameters and interactions between parameters of a steady-state 1-D neutron transport equation in planar geometry. Based on the screening results, we construct a reduced-order model which depends on significantly fewer parameters and therefore has less degrees of freedom. The resultant reduced-order model accurately characterizes the nonlinear relations between 14 physical parameters and the scalar flux. The reduced-order representation makes it computationally feasible to analyze the sensitivity of the model parameters without using Monte Carlo simulations which are often time consuming.

In the future, we will apply the algorithm to the angular flux which is a more appropriate response of the model. Since the cross sections can change significantly as the energy level changes, it is also important to consider multiple energy groups. The transport equation considered in this report does not involve fission which is an important source of reaction. This will be addressed in the future work. The 1-D planar geometry considered here is only valid when the cross sections, internal source are independent of the other two directions (y and z). 3-D transport equation will be analyzed for more realistic situations. Finally, we will investigate the implementation of this algorithm in DENOVO.

Section 3: A gradient-based high-dimensional model reduction

Introduction:

The behavior of a nuclear reactor is determined by the flow of neutrons through the reactor core, which is modeled by the Boltzmann transport equation. The solution depends on a large number of cross-section parameters that describe the way various types of materials (i.e. nuclear fuel, control rods, coolant etc.) interact with the neutrons. The cross-section are measured experimentally and hence there is uncertainty associated with their values. Of particular interest is the case when the uncertainty in the parameters is relatively large, which can account for changes in the properties of nuclear material over the entire life span of the reactor as well as the buildup of crud on the fuel and control rod cladding. Furthermore, discretizations of the Boltzmann equation often result in a large number of cross-section parameters, often in the thousands and even tens of thousands, and therefore, we are forced to approximation stochastic versions of the Boltzmann system that depend on a large number of uncertain parameters. This is certainly the case in most CASL¹ challenge problems and this report explains, both theoretically and computationally, the advantages of a gradient-based model reduction approach applied to a specific radiation transport example described in below.

The classical approach to uncertainty quantification (UQ) for the neutron flow problem is to use sensitivity analysis (SA) [Cacuci, 2003]. An approximation to the first and second moment of a quantity of interest (QoI) are computed using the derivative of the QoI. The SA approach has given us many techniques for finding the derivatives (i.e. forward and adjointed methods), however, the method is suitable only for problems with small uncertainty ranges. Sampling methods like Monte Carlo (MC) [Fishman, 1996] and Stochastic Collocation (SC) [Babuška et al., 2007, Nobile et al., 2008b,a] take several realizations of the QoI for different values of the uncertain parameters and can approximate problems with arbitrary uncertainty ranges (e.g. uniform, Gaussian, etc.). However, MC approaches have very slow convergence rates and while SC method can utilize information about the derivatives, the number of samples required is still prohibitively large for extremely high-dimensional problems [Roderick et al., 2010a, Lockwood and Anitescu, 2010], rendering them computational infeasible.

Reduced Order Modeling (ROM) is a general approach that seeks to replace a physical model with an equivalent one of lower dimensions [Antoulas, 2005, Roderick et al., 2010b, Burkardt et al., 2007], however, most ROM techniques have been developed in the context of deterministic problems (i.e. control and optimization and solvers) and thus, are not directly applicable in the UQ context. The Karhunen-Loève (KL) expansion [Loève, 1977, Loève, 1978] is the most common ROM technique used in the context of stochastic problems. KL creates a low dimensional approximation to the uncertainty, however, KL requires strong correlation between the parameters as well as explicit knowledge of the correlation function. Furthermore, the error bounds are not rigorous for non-linear and non-Gaussian problems.

In recent years, we have seen a new ROM approach for UQ within the context of neutron transport; one that combines Monte Carlo sampling with sensitivities (i.e. derivatives) of the QoI to compute a subspace that approximates the span of the gradient of the QoI [Constantine and Wang, 2012, Abdel-Khalik, 2011, Abdel-Khalik and Hite, 2011]. Consequently, the problem is

¹Consortium for Advanced Simulation of Light water reactors

projected onto the resulting low dimensional subspace allowing for the application of SC or MC techniques. While the results are promising, this new approach suffers from the lack of rigorous error bounds that relate the error in the approximation of the gradient to the error in the statistics of the QoI. Convergence is assumed rather than proven, especially in the case when the parameters have complex probability distributions (i.e. non-Uniform and non-Gaussian).

In this work, we develop a generalized framework for gradient based ROM approach for high dimensional UQ. Our results apply to linear and non-linear QoIs, large range for the uncertainty in the random input parameters as well as general probability distributions. The CASL challenge problem we solved involves neutron transport with uncertainty in the cross sections. We look for the effective dimension of the problem, that is a subspace of the uncertainty domain, so that we can project the problem onto that subspace and preserve the statistics of the QoI. We prove rigorous error bounds that apply to problems with general probability distributions.

Problem definition:

We consider the 1-D Boltzmann neutron transport equation

$$\frac{\partial \psi}{\partial t}(t, x, \theta) + \cos(\theta) \frac{\partial \psi}{\partial x}(t, x, \theta) + \sigma_t(x) \psi(t, x, \theta) = \sigma_s(x) \phi(t, x) + \nu \sigma_f(x) \phi(t, x) + f(t, x),$$

where

- $\psi(t, x, \theta)$ is the density of neutrons at time t , location x moving in direction θ ;
- $\phi(t, x) = \int_0^{2\pi} \frac{\psi(t, x, \theta)}{2\pi} d\theta$ is the total number of neutrons at time t and location x ;
- $f(t, x)$ is the external source and ν is the average number of neutron emitted after a fission reaction;
- $\sigma_t(x)$, $\sigma_s(x)$ and $\sigma_f(x)$ are the total, scatter and fission cross sections.

To exhibit the theoretical results we consider a mockup reactor problem consisting of two fuel rods placed on the two sides of a control rod and coolant medium in between, see Figure 1. We introduce uncertainty in the cross sections in the form of additive white noise field that is sampled from a truncated Gaussian distribution. That is

$$\sigma_t(x; \eta_t) = \bar{\sigma}_t(x) + \eta_t, \quad \sigma_s(x; \eta_s) = \bar{\sigma}_s(x) + \eta_s \quad \text{and} \quad \sigma_f(x; \eta_f) = \bar{\sigma}_f(x) + \eta_f,$$

where $\eta_t = \eta_s + \eta_f + \eta_c$. We define the QoI as the reactor criticality given by the solution to the eigenvalue problem

$$\cos(\theta) \frac{\partial \psi}{\partial x}(x, \theta) + \sigma_t(x; \eta_t) \psi(x, \theta) - \sigma_s(x; \eta_s) \phi(x) = \frac{\nu}{k} \sigma_f(x; \eta_f) \phi(x). \quad (1)$$

Let $k = Q(\eta)$, where $\eta = (\eta_s, \eta_f, \eta_c) \in \mathbb{R}^N$, where N is high-dimensional, be a random vector with probability distribution $\rho(\cdot)$. Then, our goal is to compute the expected value of the QoI $Q(\cdot)$, i.e.

$$E[Q(\cdot)] = \int Q(\eta) \rho(\eta) d\eta. \quad (2)$$

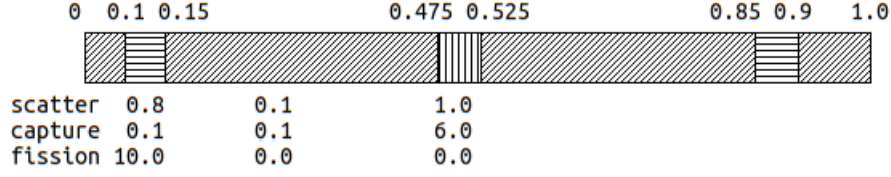


Figure 1: Mockup reactor problem

We seek to decompose \mathbb{R}^N into “active” and “passive” subspaces U_a and U_p so that we can project (2) as

$$E[Q(\cdot)] = \int Q(\eta)\rho(\eta)d\eta \approx \int_{U_a} Q(\eta_a)\hat{\rho}(\eta_a)d\eta_a, \quad (3)$$

where $\hat{\rho}(\eta_a) = \int_{U_p} \rho(\eta_a + \eta_p)d\eta_p$ is a transformed probability measure. Using the adjoint method, we compute an approximation to the gradient of $Q(\eta)$ and we use that information to form U_a and U_p . Next we describe some theoretical results and outline the algorithm used to define these subspaces.

Theoretical Results:

We prove the following sufficient condition for the error associated with the projection (3).

Theorem 1 (Gradient Bound) *Let subspaces U_a and U_p be orthogonal complements of each other. Suppose there exists a probability density function $g(\eta)$ defined on \mathbb{R}^N that satisfies*

$$|\langle \nabla Q(\eta_a + s\eta_p), \eta_p \rangle| \rho(\eta_a + \eta_p) \leq \epsilon g(\eta_a + \eta_p), \quad \forall \eta_a \in U_a, \forall \eta_p \in U_p, \forall s \in [0, 1]. \quad (4)$$

Then we have the bounds

$$\begin{aligned} \|Q(\eta) - Q(F_{U_a}\eta)\|_{L^1_{\rho(\cdot)}(\mathbb{R}^N)} &= \int |Q(\eta) - Q(F_{U_a}\eta)|\rho(\eta)d\eta \leq \epsilon, \\ \left| \int Q(\eta)\rho(\eta)d\eta - \int_{U_a} Q(\eta_a)\hat{\rho}(\eta_a)d\eta_a \right| &\leq \epsilon, \end{aligned}$$

where F_{U_a} is the projection operator $\mathbb{R}^N \rightarrow U_a$ and $\hat{\rho}(\eta_a) = \int_{U_p} \rho(\eta_a + \eta_p)d\eta_p$.

Note that this result is an extension of classical KL expansion to non-linear problems with a general probability distribution. Next, we explain the sampling based approach for forming U_a^k and U_p^k that will approximate condition (4).

Algorithm 1 (Approximate Passive Subspace) *Let $U_p^0 = \mathbb{R}^N$, $U_a^0 = \{0\}$ and $d_0 = 0$. Then iterate for $k = 1, 2, \dots$*

1. Sample η_k as a random vector with probability density $\rho(\cdot)$.
2. Compute $\nabla Q(\eta_k)$.

3. If condition (4) is satisfied for $\nabla Q(\eta_k)$ with U_p^{k-1} , U_a^{k-1} , then use $U_p^k = U_p^{k-1}$ and $U_a^k = U_a^{k-1}$ and increment $d_k = d_{k-1} + 1$.
4. If condition (4) is not satisfied, let H be the matrix with columns $\{\eta_i\}_{i=1}^k$, then define U_a^k to be the space spanned by the dominant left singular vectors of H associated with the singular values with magnitude more than ϵ . Let $d_k = 0$.
5. If d_k is sufficiently large, stop the iteration and use projection (3) with $U_a = U_a^k$ and $U_p = U_p^k$ to reduce the dimension of the problem.

Note that step 4 is contingent upon the choice of $\rho(\cdot)$. For a more complex probability distribution, the condition may have to be modified. Algorithm 1 is a probabilistic approach with non-zero probability of failure. Let e_k be the error associated with projection (3) at step k , then we get the following two bounds:

Theorem 2 (Probability of Failure) *There exists a sequence $\{m_k\}$ with $0 \leq m_k \leq 1$, so that*

$$P(e_k > \epsilon) \leq (1 - m_k)^{d_k}.$$

Furthermore, there exists n so that if $k < n$ then $m_k = 0$ and if $k \geq n$ then $m_k > 0$.

Theorem 3 (Error Distribution) *Suppose $e_k > \epsilon$, then the mean and variance of e_k are bounded by:*

$$E[e_k - \epsilon] \leq \frac{C}{d_k + 1}, \quad V[e_k - \epsilon] \leq \frac{C^2}{(d_k + 1)^2}.$$

Numerical Results:

We consider the problem of estimating the expected value for the reactor criticality. We discretize the operators (1) using a uniform grid with $M = 1000$ nodes, the convection operator is approximated by finite difference unwinding scheme and $\phi(x)$ is approximated by a 4 point quadrature on the unit disk. The resulting problem has $4 \times 1000 = 4000$ degrees of freedom with the dimension $N = 3 \times 1000 = 3000$ for the uncertain domain.

Using spacial discretization of 1000 points, the size of the problem is small enough to allow us to compare the results from Algorithm 1 to Monte Carlo sampling applied to the full order model. In Figure 2 we see the three modes associated with each type of nuclear reaction. We see that the problem is most sensitive with respect to the uncertainty in the capture and fission cross sections at the locations of the fuel and control rods.

Using 1.2×10^4 samples, we compute the expected value of k to be 1.0003, i.e. the reactor is critical to within numerical error. Since the our numerical scheme is first order in space, we only consider three digits of accuracy. Let $\epsilon = 10^{-3}$ and apply Algorithm 1. The results are shown in table below. This example illustrate the advantage of applying this technique to the CASL challenge problem described above. Here we are able to approximate the $N = 3000$ dimensional problem by using an active subspace of dimension 3 and approximate (2) accurately with only 50 MC samples.

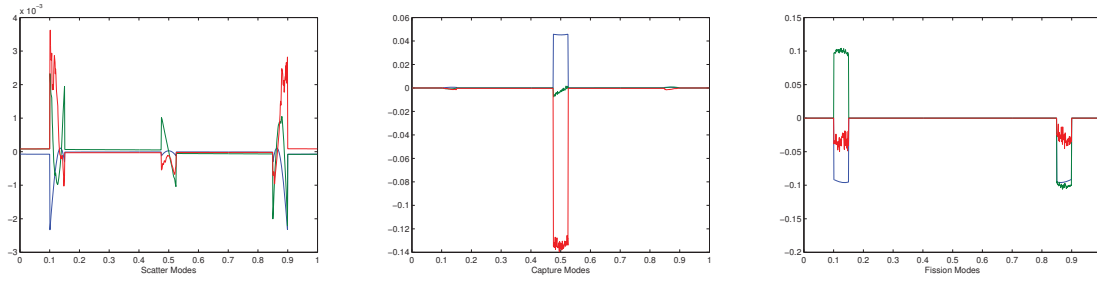


Figure 2: The three modes of U_a^{50} associated with the scatter (left), capture (center) and fission (right) cross-sections.

Model type	$E[Q(\cdot)]$	Dimension	# samples
Full order	1.0003	3000	$1.2e + 4$
ROM	1.0001	3	50

Bibliography:

H. S. Abdel-Khalik. On Non-linear Reduced order Modeling. International Conference on Mathematics and Computational Methods Applied to Nuclear Science and Engineering, 2011.

H. S. Abdel-Khalik and J. M. Hite. Reduced Order Modeling: Tensor-Free Expansion for Nonlinear Features Identification. Transactions of the American Nuclear Society, 104, 2011.

A. C. Antoulas. Approximation of Large-Scale Dynamical Systems. SIAM, 2005. I. Babuška, F. Nobile, and R. Tempone. A stochastic collocation method for elliptic partial differential equations with random input data. SIAM J. Numer. Anal, 43(3):1005–1034, 2007.

J. Burkardt, M. Gunzburger, and C. G. Webster. Reduced order modeling of some nonlinear stochastic partial differential equations. International Journal of Numerical Analysis and Modeling, 4(3-4):368–391, 2007.

Bang, Y.S., Abdel-Khalik, H.S. and Hite, J.M., “Hybrid Reduced Order Modeling Applied to Nonlinear Models”, *International Journal for Numerical Methods in Engineering*, Vol. 91, Issue 9, (2012a); pp. 929–949.

Campolongo, F., & Saltelli, A. (1997). Sensitivity analysis of an environmental model: an application of different analysis methods. *Reliability Engineering System Safety*, 57, 49–69.

D. G. Cacuci. Sensitivity and Uncertainty Analysis. Chapman & Hall/CRC, 2003. ISBN 1-58488-115-1.

Cao, Y., Chen, Z., & Gunzburger, M. (2009). ANOVA expansions and efficient sampling methods for parameter dependent nonlinear PDEs. *Inter. J. Numer. Anal. Model*, 6, 256–273.

P. G. Constantine and Q. Wang. Input Subspace Detection for Dimension Reduction in High Dimensional Approximation. eprint arXiv:1202.3508, Feb 2012.

Devaney, J. J., Bordwell, L. O., & Devaney, M. J. (1962). *Hafnium cross sections and their temperature dependence*. Los Alamos.

G. Fishman. Monte Carlo: Concepts, algorithms, and applications. Springer Series in Operations Research. Springer-Verlag, New York, 1996. ISBN 0-387-94527-X.

Gunzburger, M., & Labovsky, A. (2012). An efficient and accurate numerical method for high-dimensional stochastic PDEs. *SIAM Journal of Scientific Computing*.

Hu, Z., & Smith, R. C. (2013). Identification of most influential parameters in the homogenized energy model for macro-fiber composite actuators using high-dimensional model reduction. *Submitted to the 2013 American Control Conference*.

Li, G., Rosenthal, C., & Rabitz, H. (2001). High dimensional model representations. *J. Phys. Chem. A*, 105(33), 7765-7777.

Li, G., Wang, S.-W., Rabitz, H., Wang, S., & Jaffe, P. (2002). Global uncertainty assessments by high dimensional model representations (HDMR). *Chemical Engineering Science*, 57, 4445-4460.

B. A. Lockwood and M. Anitescu. Gradient-Enhanced Universal Kriging for Uncertainty Propagation. Technical Report MCS-P1808-1110, Argonne National Lab, 2010.

Ma, X., & Zabarar, N. (2010). An adaptive high-dimensional stochastic model representation technique for the solution of stochastic partial differential equations. *J. of Computational Physics*, 229, 3884-3915.

M. Loeve. Probability theory. I. Springer-Verlag, New York, fourth edition, 1977. Graduate Texts in Mathematics, Vol. 45.

M. Loeve. Probability theory. II. Springer-Verlag, New York, fourth edition, 1978. ISBN 0-387-90262-7. Graduate Texts in Mathematics, Vol. 46.

Morris, M. (1991). Factorial sampling plans for preliminary computational experiments. *Technometrics*, 33(2), 161-174.

F. Nobile, R. Tempone, and C. G. Webster. An anisotropic sparse grid stochastic collocation method for partial differential equations with random input data. *SIAM J. Numer. Anal.*, 46(5):2411–2442, 2008a.

F. Nobile, R. Tempone, and C. G. Webster. A sparse grid stochastic collocation method for partial differential equations with random input data. *SIAM J. Numer. Anal.*, 46(5):2309–2345, 2008b.

Rabitz, H., & Alis, O. F. (1999). General foundation of high dimensional model representations. *J. Math. Chem.*, 25, 197-233.

Rabitz, H., Alis, O. F., Shorter, J., & Shim, K. (1999). Efficient input—output model representations. *Comput. Phys. Comm.*, 117, 11-20.

O. Roderick, M. Anitescu, and P. Fischer. Polynomial Regression Approaches Using Derivative Information for Uncertainty Quantification. *Nuclear Science and Engineering*, 164:122–139, 2010a.

O. Roderick, Z.Wang, and M. Anitescu. Dimensionality Reduction for Uncertainty Quantification of Nuclear Engineering Models . Technical Report MCS-P1832-0111, Argonne National Lab, 2010b.

Shorter, J., Precila, C. I., & Rabitz, H. (1999). An efficient chemical kinetics solver using high dimensional model representations. *J. Phys. Chem. A*, 103(36), 7192- 7198.

Sobol, I. M. (1993). Sensitivity analysis for non-linear mathematical model. *Math. Modelling Comput. Exp.*, 1, 407-414.

Sobol, I. M. (2003). Theorems and examples on high dimensional model representation. *Reliab. Eng. Syst. Safety*, 79, 187-193.

Sood, A., Forster, R. A., & Parsons, D. K. (2003). Analytical benchmark test set for criticality code verification. *Progress in Nuclear Energy*, 42(1), 55-106.

Wang, S. W., Levy II, H., Li, G., & Rabitz, H. (1999). Fully equivalent operational models for atmospheric chemical kinetics within global chemistry-transport models. *J. Geophys. Res.*, 104(D23), 30417-30426.

Appendix:

We discuss here the construction of both first- and second-order sample matrices as well as how to calculate the first- and second-order effects using the sampling matrices.

We first illustrate the construction of a level q sampling matrix B^* for k -th dimensional factor vector $\vec{x} = \{x_i\}_{i=1}^k$. Here q is a positive integer, and x_i 's are integers on the interval $[0, q-1]$. A linear mapping will map \vec{x} to the actual variables \vec{p} in the function $f(\vec{p})$; e.g., $p_i = lb_i + x_i(ub_i - lb_i)/(q-1)$, where lb_i and ub_i are respectively the lower bound and upper bound of p_i . Note that our goal is to construct a matrix B^* has dimensions $(k+1) \times k$ and there are two rows that differ only in their i -th entries for $i=1, 2, \dots, k$.

1. Construct a matrix B : strictly lower triangular of one's with size $(k+1) \times k$.

$$B = \begin{pmatrix} 0 & 0 & 0 & \dots & 0 \\ 1 & 0 & 0 & \dots & 0 \\ 1 & 1 & 0 & \dots & 0 \\ \vdots & \vdots & \vdots & \ddots & \vdots \\ 1 & 1 & 1 & \dots & 0 \end{pmatrix}$$

2. Select the increment Δ for the components of \vec{x} . Δ is a positive integer and $\Delta < q-1$. Morris (Morris, 1991) suggests taking $\Delta < q/2$.
3. Randomly pick a starting vector \vec{x}^* from set $\{0, 1, 2, q-1-\Delta\}$.
4. Define a matrix D^* , k -dimensional diagonal matrix of integers, whose elements are selected from the set $\{-1, 1\}$ with equal probability.
5. Calculate B^* : $B^* = (J_{k+1,1} \vec{x}^* + \Delta/2[(2B - J_{k+1,k})D^* + J_{k+1,k}])P^*$, where $J_{m,n}$ is a $m \times n$ matrix of one's, P^* is a $k \times k$ random permutation matrix, i.e., a matrix obtained by randomly permuting columns of a $k \times k$ identity matrix.

To evaluate $\{d_{ss}^t\}_{s=1}^k$ in step 2 of *Algorithm 1*, let the i -th row of B_i^* be $B_i^*(i) = [b_{i1}^t, b_{i2}^t, \dots, b_{is}^t, \dots, b_{ik}^t]$ which is different from the j -th row of B_i^* only at s -th entry; i.e., $B_i^*(j) = [b_{i1}^t, b_{i2}^t, \dots, b_{js}^t, \dots, b_{ik}^t]$. Then the first-order elementary effect for the s -th component is defined as

$$d_{ss}^t = \left| \frac{f(B_i^*(i)) - f(B_i^*(j))}{b_{is}^t - b_{js}^t} \right|.$$

Inspired by the second-order sampling matrix, we construct a level q second-order sampling matrix A^* with dimensions $k \times k$. Note that A^* has two rows that differ only in their i -th and j -th entries for $i, j = 1, 2, \dots, k$.

1. Construct a matrix A : a $k \times k$ matrix that is composed of an $(k-1) \times (k-1)$ identity matrix, and whose first row is 0 and elements $2-k$ in the first column is 1.

$$A = \begin{pmatrix} 0 & 0 & 0 & \dots & 0 \\ 1 & 1 & 0 & \dots & 0 \\ 1 & 0 & 1 & \dots & 0 \\ \vdots & \vdots & \vdots & \ddots & \vdots \\ 1 & 0 & 0 & \dots & 1 \end{pmatrix}$$

2. Define a matrix D^* , k -dimensional diagonal matrix of integers, whose elements are selected from the set $\{-1,1\}$ with equal probability.
3. Calculate A^* : $A^* = (J_{k,1}\bar{x}^* + \Delta/2[(2A - J_{k,k})D^* + J_{k,k}])P^*$, where $J_{m,n}$ and P^* are defined previously.

To evaluate $\{d_{sv}^l\}_{s,v=1}^k$ in step 4 *Algorithm 1*, let us assume that the m -th row of A_t^* , $A_t^*(m) = [b_{m1}^l, \dots, b_{ms}^l, \dots, b_{mv}^l, \dots, b_{mk}^l]$, is different from the n -th row of A_t^* only at the v -th and the s -th entries; i.e., $A_t^*(n) = [b_{n1}^l, \dots, b_{ns}^l, \dots, b_{nv}^l, \dots, b_{nk}^l]$. Then the second-order elementary effect between the v -th and the s -th components is defined as

$$d_{sv}^l = \left| \frac{f(A_t^*(m)) - f(b_{m1}^l, \dots, b_{ms}^l, \dots, b_{nv}^l, \dots, b_{mk}^l)}{(b_{ms}^l - b_{ns}^l)(b_{mv}^l - b_{nv}^l)} - \frac{f(b_{m1}^l, \dots, b_{ns}^l, \dots, b_{mv}^l, \dots, b_{mk}^l) - f(A_t^*(n))}{(b_{ms}^l - b_{ns}^l)(b_{mv}^l - b_{nv}^l)} \right|.$$